Engineered Science
DOI: https://dx.doi.org/10.30919/es1016

Investigation of Sandwich-Type Generator Thermoelectric Element Power Generation

Catur Harsito,[1,*] Ganjar Pramudi,[1] Riyadi Muslim,[1] Dimas Adika[1] and Yudi Kurniawan[2]

Abstract

Energy needs and awareness of renewable energy are always increasing from year to year. This results in a very large demand for renewable energy. Nowadays, its special concern is exhaust emissions. This article presents numerical thermoelectric modeling and simulation with BiTe-based materials. The type of sandwich material and the height of the thermoelectric legs are varied for the output power and power efficiency factor. Numerical simulations are carried out using software assistance. The input temperature on the thermoelectric hot side varied from 300-1000 K. A simplification of the simulation was carried out by taking into account thermoelectricity with a single leg (a couple n-type and p-type). Based on the analysis, the choice of sandwich material has an effect on the temperature gradient and the output power of the BiTe-based thermoelectric generator. The resulting power output is 32.82 mW, and the maximum efficiency is 22.92% when the temperature difference is 350–400 K. The results show that the developed generator can be used at temperatures below 600K.

Keywords: Thermoelectric generator; Sandwich-type; Efficiency; Renewable energy.
Received: 15 May 2023; Revised: 09 September 2023; Accepted: 15 September 2023.
Article type: Research article.

1. Introduction

The demand for energy grew by 40% in 2020, and is expected to continue to increase.[1,2] Based on data from the Minister of Energy and Mineral Resources, the intensity of final energy consumption per Capita in 2020 was 3.11 BOE per Capita and in 2021 it increased to 3.12 BOE per Capita and in 2022 it became 3.04 BOE per Capita.[3] The demand for electricity use causes a lot of electrical energy to be met. On the other hand, fossil energy is increasingly depleting. As one answer to this need, thermoelectric technology is an alternative source of energy. A thermoelectric device converts energy and functions as a generator as a result of temperature differences.[4] Besides functioning as a generator, this device can also be used as a heat pump and cooler. As a waste energy harvester and converter, thermoelectric is a desirable alternative when the temperature difference between the hot and cold sides is quite high. This energy conversion is a fundamental coupling between the electric charge and the energy carried by each moving electron.[5] The coupling strength of this device is called the Seebeck coefficient, or thermoelectric power.[6] The Seebeck effect is used by this device's generator function to transform heat energy into electrical energy.[7,8] The thermoelectric system has a performance that is usually assessed based on the figure of merit.[9] This non-dimensional value is denoted by ZT, which is a combination of the thermal and electrical transport properties of the system and the coupling at temperature (T).

This thermoelectric generator has several features, such as high reliability and durability at a lower cost, does not require maintenance, and has a shorter process because the energy conversion that occurs takes place without an intermediate energy conversion process.[10,11] In addition, this system has the potential to be an alternative energy source by utilizing energy waste, creating clean, emission-free, and noise-free electricity, and reducing gas and carbon emissions from the greenhouse effect.[12] This device has been widely used in portable electronic devices such as glucose monitoring device,[13] electroencephalography (EEG),[14] accelerometer,[15] sweat conductivity monitoring,[16] pressure temperature Sensor,[17] and human motion monitoring,[18] whose power requirement is

[1] *Mechanical Engineering of Vocational School, Universitas Sebelas Maret, 57126, Indonesia.*
[2] *Mechanical Engineering, Balikpapan State Polytechnic, 76129, Indonesia.*
**Email:* catur_harsito@staff.uns.ac.id (C. Harsito)

in the range of mW to μW.

There have been many developments in thermoelectric material research, Rafal Zybala[19] modified the GeTe material by adding $AgSbSe_2$ and $AgSbTe_2$ to reduce the thermal conductivity value. The results show the optimal value of ZT=1.2 at 600 K. Liu *et al*.[20] modified one of the N-type legs by adding PbTe elements. The results show a ZT value of 1.5 at a temperature of 773K. The thermoelectric thermal conductivity was reduced by adding $AgSb_2$ to SnSe, the results showed a ZT value of 1.21 at 660K. Zhongliang conducted research on the BiTe material used on P-type and N-type, the resulting efficiency was 17% at 500K.[21] Based on several existing studies, each material has advantages at different operational temperatures. Kim, Mukyung conducted research on combining two materials to increase efficiency.[22] As explained earlier, thermoelectric have been widely used. However, there is still a lot of development and potential to increase the efficiency and output power produced.

Thermoelectric fabrication has been widely carried out.[23] Apart from that, experimental research has also been carried out, this research requires a lot of costs both for production and the test equipment used. So alternative simulations emerge to reduce research costs.[24–26] The simulation is carried out by making a thermoelectric model in 3 (dimensional) form which is then transferred into the simulation software. The simulation is carried out using Ansys software.

This paper presents 3D modeling and simulation of thermoelectric sandwich materials with p-type and n-type BiTe based thermoelectric legs. BiTe has special properties so this material is very good to use as a basic material. BiTe has a high thermoelectric efficiency value but has limitations at low operating temperatures, namely in the range of 300-600 K.[27] So this article uses two materials to increase operational temperature. The height of the thermoelectric legs and material variations are analyzed. In addition, the generated thermoelectric voltage, current, output power, and thermoelectric efficiency are calculated and analyzed using modeling and simulation.

2. Theory and methods

2.1 Theory

To carry out a numerical simulation study, we firstly found out the analytical solution to the one-dimensional thermoelectric problem with a number of n feet and the resistance R_L as an external load. The thermoelectric pair consists of a p-leg element and an n-leg element. In this study, all heat transfer losses, electrical contact resistance, and thermal contact are ignored. The system is in a stable state, and the power absorbed on the hot side of the thermoelectric module and the power released on the cold side can be expressed in the following equation.[21,28,29]

$$P_h = n\left[IT_h\alpha - \frac{1}{2}I^2R + K(T_h - T_c)\right] \quad (1)$$

$$P_h = n\left[IT_h\alpha - \frac{1}{2}I^2R + K(T_h - T_c)\right] \quad (2)$$

In the equation above, the first term is the resultant Peltier heat (power), followed by the Joule heat (power) in the second and third terms, and the Fourier (power) in the last term. The ½ ratio in the Joule heat term is an illustration that each hot junction and cold junction "consume" half of the total Joule heat because the thermoelectric module has the same number of negative legs and positive legs. The Seebeck coefficient α, resistance of a thermocouple R and thermal conductance K can be written more explicitly as

$$\alpha = (\alpha_p - \alpha_n) \quad (3)$$

$$R = \frac{\rho_p L}{A_p} + \frac{\rho_n L}{A_n} \quad (4)$$

$$K = \frac{1}{L}(K_p A_p + K_n A_n) \quad (5)$$

The length of the thermoelectric leg is indicated by L, and the cross-sectional area of the thermoelectric is indicated by A. As the difference between P_h and P_c, the output power of the system can be expressed in terms of current and external load resistance R_L. Also, the current in the system is equal to the Seebeck coefficient divided by the total resistance, where the total resistance is internal R plus external R_L.

$$P_h - P_c = W = I^2R_L \quad (6)$$

$$I = \frac{\alpha(T_h - T_c)}{R + R_L} \quad (7)$$

Based on equations (1), (2), (6) and (7), the value of the thermoelectric efficiency can be represented as,

$$\eta = \frac{P_h - P_c}{P_h} = \eta_c \frac{\beta}{(1-\beta)+(1+\beta)^2.(ZT_h)^{-1} - \eta_c/2} \quad (8)$$

Where, $\beta = \frac{R_L}{R}$, $Z = \frac{\alpha^2}{RK} = \frac{\alpha^2}{\rho\kappa}$ (when referring to a single leg with sole TE material) and $\eta_c = \frac{T_h - T_c}{T_h}$. It can be shown that the maximum efficiency occurs at $\beta = \frac{R_L}{R} = \sqrt{1 + Z\bar{T}}$, Where $\bar{T}$ is the average of T_h and T_c.

$$\eta_{max} = \frac{T_h - T_c}{T_h}\left[\frac{\sqrt{1+Z\bar{T}} - 1}{\sqrt{1+Z\bar{T}} - \frac{T_c}{T_h}}\right] \quad (9)$$

2.2 Methods

The research method used in this study was numerical prediction with the help of Ansys software.[25,30] The three-dimensional design of the thermoelectric module was made using Solidworks software and then imported into Ansys as a

Table 1. Module dimension.

Module Dimension	Value (mm)	Symbol
TE leg height	In Table 2	H
TE leg width	0.7	W
TE leg length	1.4	L
Spacing between legs	1.0	D
Substrate thickness	0.8	

reference for the geometry of the thermoelectric module. Dimensional details can be seen in Table 1 and the three-dimensional thermoelectric geometry is shown in Fig. 1. Modeling and analysis of the thermoelectric characteristics of this generator is simplified into a single leg. In addition, a variation of the thermoelectric leg in the form of a sandwich and also its height was carried out. The simulation variations are shown details in Table 2. In this study, the material used is divided into two types. The first type of material with positive leg BiTe and negative leg Bi_2S_3 which is then called material 1 (M1). the second type of material with a positive leg is a combination of two materials, namely (CuSe+; BiTe+) and a positive leg (Bi_2S_3- ; BiTe-) which is hereinafter called material 2 (M2).

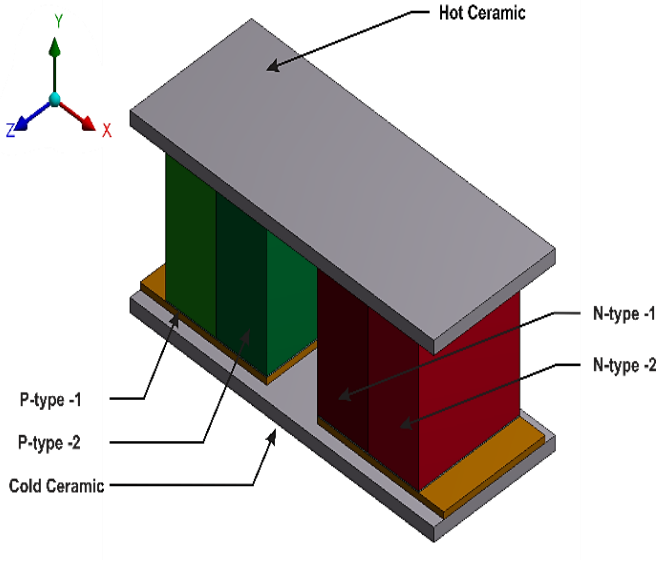

Fig. 1 Single thermoelectric geometry.

As shown in Fig. 1, this new thermoelectric model was designed by dividing the leg width into two parts. In the divided part, there are two different materials. In addition, the height of the thermoelectric leg was also evaluated to find the maximum height. In this study, the thermoelectricity was evaluated on the cold side at 300K and the hot side was varied at 300-1000K.

2.3 Meshing

The meshing results are shown in Fig. 2, where the meshing used the hexagonal method by making more detailed arrangements on parts that have small sizes to get good temperature and power distribution results. The meshing sizes used on the sides of the thermoelectric, ceramics, and copper legs are 0.1 mm, 0.05 mm, and 0.01 mm respectively.

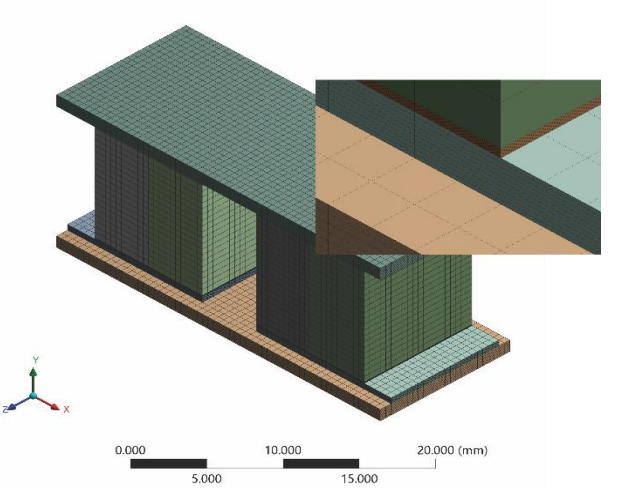

Fig. 2 Meshing model.

Table 2. Simulation variation set-up.

Material Type	Module Height (mm)	Range Hot Side (K)
(M1) (BiTe+) (Bi_2S_3-)	10	300-1000
	15	
	20	
(M2) (CuSe+; BiTe+) (Bi_2S_3-; BiTe-)	10	
	15	
	20	

2.4 Validation

Simulation research requires a validation process to verify the simulation results are running correctly. In this study, the validation process was carried out by re-simulating previous research, namely research conducted by Erturun in 2012 and also Harsito in 2020. As the basis for creating numerical models for later research activities, this method must have great precision. If this model has a maximum error value of 5%, it is considered accurate.[24,31] Based on the results of the validation carried out, it can be concluded that the modeling carried out is accurate with an error value of 1.5%. So that modeling with configurations can be continued for the simulation of this research case. An accurate validation process is also affected by a very precise mesh size.

3. Results and discussion

3.1 Power output

This section presents the simulation findings. It has been assessed how current and voltage affect the power produced. The thermoelectric performance is also evaluated by inputting

Table 3. Validation.

Variable	Erturun[31,32]	Harsito[30]	Validation
Voltage (V)	8.70E-02	8.70E-02	8.70E-02
Current Generated (mA)	328.00	326.00	326.85
Power Generated (mW)	28.50	28.00	28.44
Heat Absorbed (mW)	673.00	671.59	672.95
Efficiency (η)	4.235%	4.169%	4.226%

a hot temperature from 300 K to 1000 K while the cold temperature on the reverse side is kept constant at 289 K. According to Fig. 3, the value of the generated thermoelectric power increases with the increase in temperature difference. In addition, the combination of materials in each leg affects the value of the thermoelectric power. The length of the thermoelectric leg affects the value of the power generated. The shorter the thermoelectric leg, the higher the generated power value. However, the combination of M2 (CuSe+; BiTe+) (Bi_2S_3- ; BiTe-) material has a lower power value than M1 (BiTe+) (Bi_2S_3-) material. The power value produced at a low temperature difference is relatively similar than when the temperature difference between the hot and cold sides reaches 700 K.

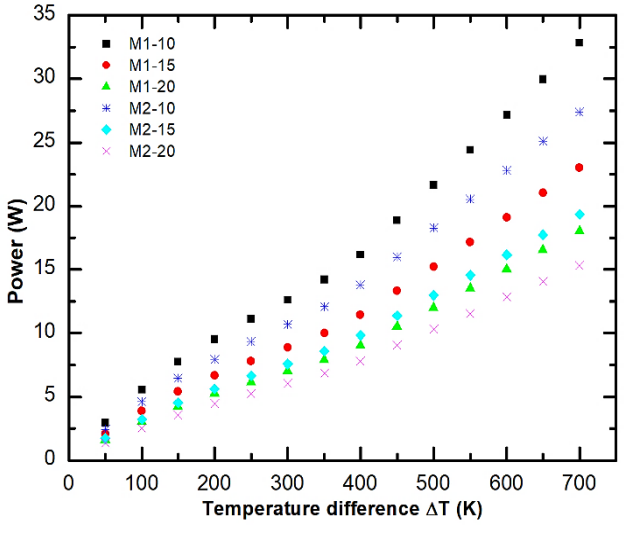

Fig. 3 Power generation and temperature difference.

As illustrated in Fig. 4, the power output value is affected by the current in the thermoelectric material. The higher the value of the applied current, the higher the value of the generated power. Based on the material used, M1 material has a higher power output value than M2 material at the same current. So that at the same power value, the value of the electric current in the M2 material is greater than that of the M1 material. As a result of variations in leg height, the power value produced by the leg height is 10mm higher than the other leg heights. This phenomenon occurs in materials M1 and M2. The higher the thermoelectric leg, the lower the power produced. This happens because the longer the leg of the module, the greater the value of its electrical resistance.[33] Apart from that, the material used also affects the value of the power produced. At the same leg length (10 mm), the power value of the M1 material is higher than the power value of the M2 material. This is caused by the influence of the thermal conductivity value; where the value of the thermal conductivity of the M2 material is a combination of the two materials so that it is 1,861 $Wm^{-1}K^{-1}$ and the M1 material is 1,280 $Wm^{-1}K^{-1}$. When the thermal conductivity is high, the thermoelectric temperature increases rapidly on the cold side, so that the thermoelectric material becomes inefficient.[21,34]

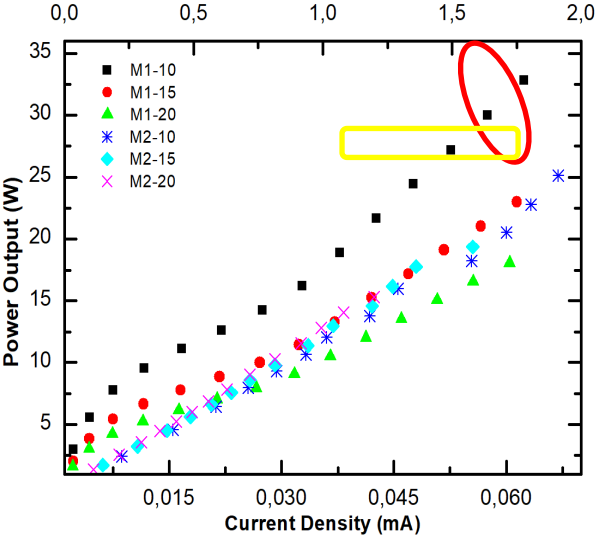

Fig. 4 Effect of current density on power output.

In addition to the current and temperature difference, the voltage generated from the thermoelectric also affects the power output. The output power value will increase along with the increase in the electric voltage value, as shown in Fig. 5. The voltage and electric current generated by the thermoelectric system are multiplied to provide the power value.[35,36]

Based on the previous discussion, differences in temperature, current and voltage affect the thermoelectric power output. These three parameters are interrelated because the value of the power output is the result of multiplying the current and voltage. In addition, the Seebeck coefficient also influences the value of the resulting voltage and current.[37] M1 material has a greater power value when the temperature

difference is greater than 200 K while M2 material will have a greater power value when the thermoelectric side temperature difference is 200 K and below.

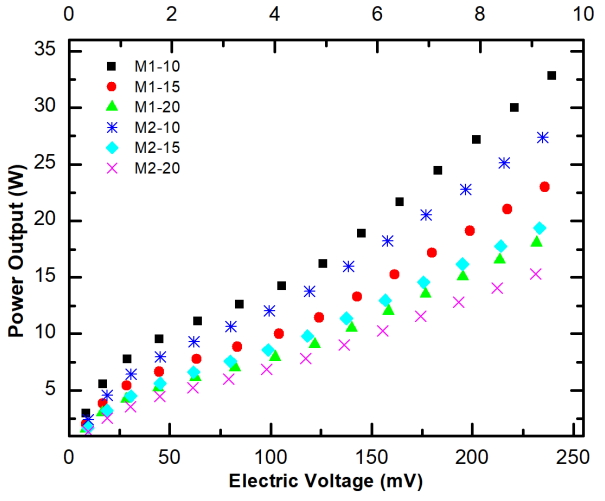

Fig. 5 Power output due to electric voltage.

3.2 Efficiency

The heat energy absorbed by a thermoelectric is then released into electrical power depending on the type of material used. Material configuration can also affect the electrical power generated. The level of thermoelectric efficiency is also influenced by the thermoelectric output voltage. Fig. 6 demonstrates that the best thermoelectric efficiency values occur when the voltage values range from 99.49 mV to 125.96 mV for Thermoelectric with a leg length of 10mm, 98.84 mV to 123.93 mV for a leg length of 15mm, and 98.06 mV to 121.78 mV for a leg length of 20mm.The maximum efficiency is produced when the difference in hot and cold temperatures is between 350-400 K for all types of materials. But the highest efficiency is in the M2 type material with a leg length of 20mm.

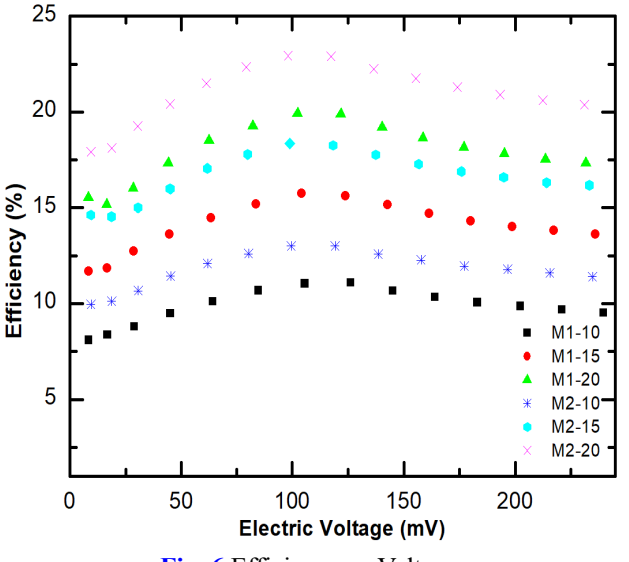

Fig. 6 Efficiency vs Voltage.

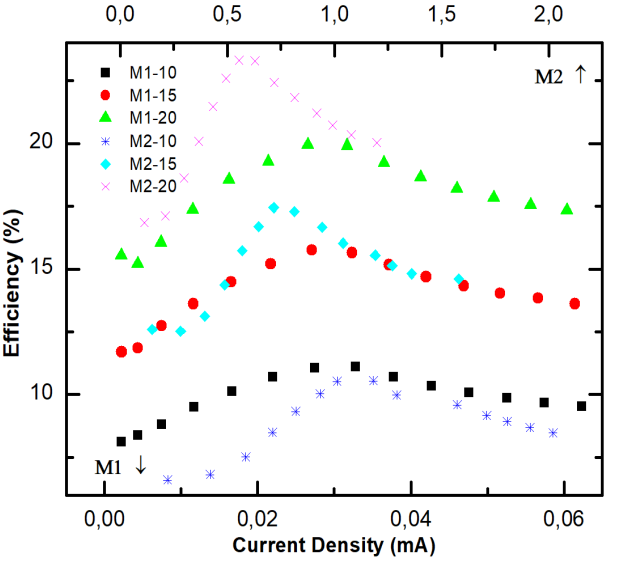

Fig. 7 Effect of current to efficiency.

The current efficiency phenomena is depicted in Fig. 7. This is the same as the relationship between voltage and efficiency because current and voltage are directly proportional to power. The maximum efficiency value is found in the M2 type material with a leg length of 20mm when the hot side is 700 K and the cold side is at 300 K.

3.3 Temperature distribution

The material that makes up this thermoelectric composite besides affecting the power generated, also affects the temperature distribution inside the material itself. The following is the result of the temperature profile on the two thermoelectric legs with two different configurations. Fig. 8 depicts the temperature distribution profile of two different types of material.

The results show that the distribution that occurs in the M1 material is more linear, in contrast to the M2 material, one of the legs has an unequal temperature distribution. The M2 material looks hot which is generated moving faster to the cold side. This results in a decrease in the value of the power released by the M2 material.

4. Conclusions

Research on numerical thermoelectric simulation of composite materials was carried out with Ansys software. Based on the simulation results, the material type M1 with a foot height of 10 mm has a power value of 32.82 mW at a temperature difference of 700K or 1000K on the hot side and 300K on the cold side. The power values of materials M1 and M2 are the same when the operating temperatures are different and the current values are different too. Different values of

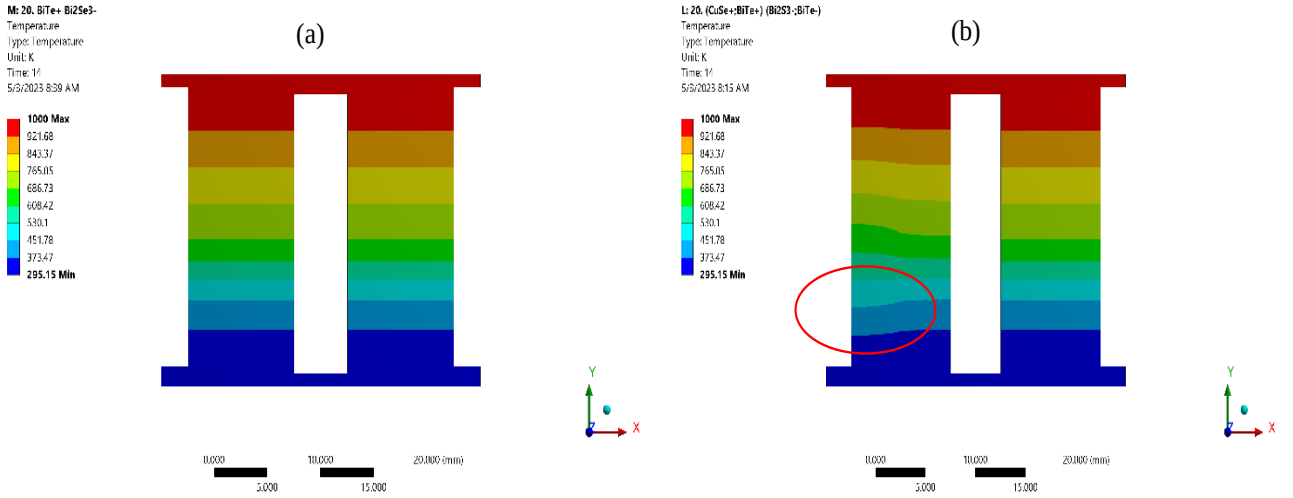

Fig. 8 Temperature Distribution (a) M1 [BiTe+; Bi_2S_3-] (b) M2 [CuSe+; BiTe+ and Bi_2S_3-; BiTe-].

thermal conductivity affect the value of this thermoelectric power. Type M2 material has an efficiency of 22.92% at a leg length of 20 mm, and the resulting power value is 6.85 mW. In research based on numerical simulations, there are several parameters that must be considered, such as the thermoelectric system. Research with a closed system to determine the effect of fixed resistance on the output power and thermoelectric efficiency can be carried out and can then be compared with one another..

Acknowledgements

The authors would like to thank the Universitas Sebelas Maret for laboratory facilities and financial assistance under the research grant project with contract number 228/UN27.22/PT.01.03/2023.

Conflict of Interest

There is no conflict of interest.

Supporting Information

Not applicable.

References

[1] D. Danardono Dwi Prija Tjahjana, Z. Arifin, S. Suyitno, W. E. Juwana, A. R. Prabowo, C. Harsito, Experimental study of the effect of slotted blades on the Savonius wind turbine performance, *Theoretical and Applied Mechanics Letters*, 2021, **11**, 100249, doi: 10.1016/j.taml.2021.100249.

[2] R. Newell, D. Raimi, G. Aldana, Global energy outlook 2019: the next generation of energy, *Resources for the Future*, 2019, **1**, 8-19.

[3] A. C. Adi, F. Lasnawatin, A.B. Prananto, L. Halim, I.G. Anutomo, D. Anggreani, F. Indarwati, M. Yusuf, L. Ambarsari, H. Yuanningrat, Handbook of Energy & Economic Statistics of Indonesia (Final Edition), Ministry of Energy and Mineral Resources Republic of Indonesia, Jakarta, 2022.

[4] C. Harsito, M. R. A. Putra, D. A. Purba, T. Triyono, Mini review of thermoelectric and their potential applications as coolant in electric vehicles to improve system efficiency, *Evergreen*, 2023, 10, 469-479, doi: 10.5109/6782150.

[5] S. Choo, F. Ejaz, H. Ju, F. Kim, J. Lee, S. E. Yang, G. Kim, H. Kim, S. Jo, S. Baek, S. Cho, K. Kim, J.-Y. Kim, S. Ahn, H. G. Chae, B. Kwon, J. S. Son, Cu_2Se-based thermoelectric cellular architectures for efficient and durable power generation, *Nature Communications*, 2021, **12**, 3550, doi: 10.1038/s41467-021-23944-w.

[6] Y. Apertet, H. Ouerdane, C. Goupil, P. Lecoeur, A note on the electrochemical nature of the thermoelectric power, *The European Physical Journal Plus*, 2016, **131**, 76, doi: 10.1140/epjp/i2016-16076-8.

[7] N. Baatar, S. Kim, A thermoelectric generator replacing radiator for internal combustion engine vehicles, *TELKOMNIKA (Telecommunication Computing Electronics and Control)*, 2011, **9**, 523-530, doi: 10.12928/telkomnika.v9i3.744.

[8] M. N. Hasan, H. Wahid, N. Nayan, M. S. Mohamed Ali, Inorganic thermoelectric materials: a review, *International Journal of Energy Research*, 2020, **44**, 6170-6222, doi: 10.1002/er.5313.

[9] A. F. Ioffe, L. S. Stil'bans, E. K. Iordanishvili, T. S. Stavitskaya, A. Gelbtuch, G. Vineyard, Semiconductor thermoelements and thermoelectric cooling, *Physics Today*, 1959, **12**, 42, doi: 10.1063/1.3060810.

[10] A. Abdul Tahrim, A. Ahmad, R. Abdul Rahim, M. S. Mohamed Ali, Characterization of heat flow in silicon nanowire arrays for efficient thermoelectric power harvesting, *Experimental Heat Transfer*, 2018, **31**, 470-481, doi: 10.1080/08916152.2018.1445674.

[11] K. V. Selvan, M. N. Hasan, M. S. Mohamed Ali, Methodological reviews and analyses on the emerging research trends and progresses of thermoelectric generators, *International Journal of Energy Research*, 2019, **43**, 113-140, doi: 10.1002/er.4206.

[12] K. Veni, Selvan, Micro-scale energy harvesting devices: review of methodological performances in the last decade,

Renewable and Sustainable Energy Reviews, 2016, **54**, 1035-1047, doi: 10.1016/j.rser.2015.10.046.
[13] H. Lee, T. K. Choi, Y. B. Lee, H. R. Cho, R. Ghaffari, L. Wang, H. J. Choi, T. Dong Chung, N. Lu, T. Hyeon, S. H. Choi, D.-H. Kim, A graphene-based electrochemical device with thermoresponsive microneedles for diabetes monitoring and therapy, *Nature Nanotechnology*, 2016, **11**, 566-572, doi: 10.1038/nnano.2016.38.
[14] T. Torfs, V. Leonov, R. F. Yazicioglu, P. Merken, C. Van Hoof, R. J. M. Vullers, B. Gyselinckx, Wearable autonomous wireless electro-encephalography system fully powered by human body heat. SENSORS, 2008 IEEE. October 26-29, 2008, Lecce, Italy. IEEE, 2008, 1269-1272, doi: 10.1109/ICSENS.2008.4716675.
[15] Yancheng, Wang, Wearable thermoelectric generator to harvest body heat for powering a miniaturized accelerometer, *Applied Energy*, 2018, **215**, 690-698, doi: 10.1016/j.apenergy.2018.02.062.
[16] L. Ortega, A. Llorella, J. P. Esquivel, N. Sabaté, Self-powered smart patch for sweat conductivity monitoring, *Microsystems & Nanoengineering*, 2019, **5**, 3, doi: 10.1038/s41378-018-0043-0.
[17] S. Han, F. Jiao, Z. U. Khan, J. Edberg, S. Fabiano, X. Crispin, Thermoelectric polymer aerogels for pressure-temperature sensing applications, *Advanced Functional Materials*, 2017, **27**, 1703549, doi: 10.1002/adfm.201703549.
[18] D. Y. Choi, M. H. Kim, Y. S. Oh, S.-H. Jung, J. H. Jung, H. J. Sung, H. W. Lee, H. M. Lee, Highly stretchable, hysteresis-free ionic liquid-based strain sensor for precise human motion monitoring, *ACS Applied Materials & Interfaces*, 2017, **9**, 1770-1780, doi: 10.1021/acsami.6b12415.
[19] Rafał, Zybała, Preparation and characterization of nanostructured $(GeTe)_{75}(AgSbTe_2)_x(AgSbSe_2)_y$ thermoelectric materials, *Synthetic Metals*, 2020, **270**, 116606, doi: 10.1016/j.synthmet.2020.116606.
[20] W. Liu, T. Hong, S. Dong, D. Wang, X. Gao, Y. Xiao, L.-D. Zhao, Synergistically optimizing carrier and phonon transport properties in n-type PbTe through I doping and SnSe alloying, *Materials Today Energy*, 2022, **26**, 100983, doi: 10.1016/j.mtener.2022.100983.
[21] Z. Ouyang, D. Li, Modelling of segmented high-performance thermoelectric generators with effects of thermal radiation, electrical and thermal contact resistances, *Scientific Reports*, 2016, **6**, 24123, doi: 10.1038/srep24123.
[22] Mikyung, Kim, Analysis of a sandwich-type generator with self-heating thermoelectric elements, *Energy Conversion and Management*, 2014, **81**, 440-446, doi: 10.1016/j.enconman.2014.02.061.
[23] A. K. Haq, J. Hendrawan, A. H. Asyari, F. Abdussalam, S. Utara, Studi Efektivitas Couple Thermoelektrik Sebagai Pendingin Prosesor, Conference on Information Technology and Electrical Engineering, Yogyakarta, 2017, 137-141.
[24] C. Harsito, T. Triyono, E. Roviyanto, Analysis of heat potential in solar panels for thermoelectric generators using ANSYS software, *Civil Engineering Journal*, 2022, **8**, 1328-1338, doi: 10.28991/cej-2022-08-07-02.
[25] C. Harsito, A. N. S. Permata, Investigation of air distribution in mosque rooms with different angles of supply and inlet velocity, *International Journal of Heat and Technology*, 2021, **39**, 1383-1388, doi: 10.18280/ijht.390439.
[26] H. Hazimi, U. Ubaidillah, R. Alnursyah, H. Nursya'bani, B. W. Lenggana, Wibowo, Improvement of space tube frame for formula student vehicle. Proceedings of the 6th International Conference and Exhibition on Sustainable Energy and Advanced Materials. Singapore: Springer Singapore, 2020: 735-744, doi: 10.1007/978-981-15-4481-1_70.
[27] M. Maksymuk, T. Parashchuk, B. Dzundza, L. Nykyruy, L. Chernyak, Z. Dashevsky, Highly efficient bismuth telluride-based thermoelectric microconverters, *Materials Today Energy*, 2021, **21**, 100753, doi: 10.1016/j.mtener.2021.100753.
[28] S. Lin, L. Zhang, W. Zeng, D. Shi, S. Liu, X. Ding, B. Yang, J. Liu, K.-H. Lam, B. Huang, X. Tao, Flexible thermoelectric generator with high Seebeck coefficients made from polymer composites and heat-sink fabrics, *Communications Materials*, 2022, **3**, 44, doi: 10.1038/s43246-022-00263-1.
[29] D. M. Rowe, Thermoelectrics Handbook: Macro to Nano, (1st ed.), CRC Press, 2006, doi: 10.1201/9781420038903.
[30] C. Harsito, T. Triyono, E. Roviyanto, Analysis of heat potential in solar panels for thermoelectric generators using ANSYS software, *Civil Engineering Journal*, 2022, **8**, 1328-1338, doi: 10.28991/cej-2022-08-07-02.
[31] Ugur, Erturun, Influence of leg sizing and spacing on power generation and thermal stresses of thermoelectric devices, *Applied Energy*, 2015, **159**, 19-27, doi: 10.1016/j.apenergy.2015.08.112.
[32] U. Erturun, K. Mossi, A feasibility investigation on improving structural integrity of thermoelectric modules with varying geometry, *Proceedings of ASME 2012 Conference on Smart Materials, Adaptive Structures and Intelligent Systems*, September 19-21, 2012, Stone Mountain, Georgia, USA. 2013, 939-945, doi: 10.1115/SMASIS2012-8247.
[33] N. R. F. Putra, M. S. Muntini, D. Anggoro, Pemodelan Dan fabrikasi modul thermoelectric generator (TEG) berbasis semikonduktor Bi_2Te_3 dengan metode penyusunan thermoelement untuk menghasilkan Daya listrik, *Jurnal Sains Dan Seni ITS*, 2019, **7**, 51-58, doi: 10.12962/j23373520.v7i2.36722.
[34] P. Ying, R. He, J. Mao, Q. Zhang, H. Reith, J. Sui, Z. Ren, K. Nielsch, G. Schierning, Towards tellurium-free thermoelectric modules for power generation from low-grade heat, *Nature Communications*, 2021, **12**, 1121, doi: 10.1038/s41467-021-21391-1.
[35] W.-D. Liu, L. Yang, Z.-G. Chen, J. Zou, Promising and eco-friendly Cu_2X-based thermoelectric materials: progress and applications, *Advanced Materials*, 2020, **32**, 1905703, doi: 10.1002/adma.201905703.
[36] D. W. Kim, J. H. Lee, J. K. Kim, U. Jeong, Material aspects of triboelectric energy generation and sensors, *NPG Asia Materials*, 2020, **12**, 6, doi: 10.1038/s41427-019-0176-0.
[37] X. Wang, H. Wang, W. Su, T. Wang, M. A. Madre, J. Zhai, T. Chen, A. Sotelo, C. Wang, A novel multilayer composite

structured thermoelectric module with high output power, *Journal of Materials Chemistry A*, 2020, **8**, 3379-3389, doi: 10.1039/c9ta13881a.